Available online at www.sciencedirect.com
SCIENCE DIRECT®
Chemical Physics Letters 385 (2004) 233–238
CHEMICAL PHYSICS LETTERS
www.elsevier.com/locate/cplett

Photoexcitation of the NO dimer below the threshold of the $NO(A^2\Sigma^+) + NO(X^2\Pi)$ channel: a photoion and photoelectron imaging study

V. Dribinski, A.B. Potter, I. Fedorov, H. Reisler *

Department of Chemistry, University of Southern California, Los Angeles, CA 90089-0482, USA

Received 21 October 2003; in final form 12 December 2003
Published online: 19 January 2004

Abstract

The photoexcitation of $(NO)_2$ at 242–221 nm is studied by photoion and photoelectron imaging. A broad and structureless absorption band starting at $41{,}300 \pm 300$ cm^{-1} is observed. Ionization via the excited state accesses predominantly a dissociative state of $(NO)_2^+$. The broad kinetic energy distribution of the photoelectrons suggests that the excited state has a large valence component in the Franck–Condon region, and that the geometries of the excited neutral state and the dimer ion state differ markedly. We propose that the same 'bright' state of mixed valence/Rydberg character is accessed at 242–200 nm, in agreement with preliminary ab initio calculations.

1. Introduction

The ultraviolet (UV) spectroscopy, photophysics, and photochemistry of the NO dimer, a weakly covalently bound molecule, have attracted considerable attention recently. The ground state of the dimer is formed via the bonding interaction of two NO radicals; however, since the monomers have their unpaired electrons in antibonding π^* orbitals, the N–N bond is rather weak, 710 ± 10 cm^{-1} [1,2]. Electronic structure calculations reveal that many of the dimer's excited states have no counterpart in the electronically excited states of the monomers. For example, there are eight electronic states in the energy region up to 1 eV above the ground state, whose characterization has been a great challenge to theory [3,4]. To date, no direct experimental observation of these low-lying states has been reported. The situation regarding the higher-lying electronic states is reversed. While experiments show the existence of at least one very strong and broad absorption band in the UV that peaks at ~205 nm [5,6], a theoretical characterization of this state(s) is yet to be published. Following absorption at 223–193 nm, the excited NO dimer dissociates, giving rise to $NO(X^2\Pi) + NO(A^2\Sigma^+)$. In addition, the $NO(X^2\Pi) + NO(B^2\Pi)$ channel was observed at 193 nm [7,8].

The published absorption spectra of the dimer have been obtained with thermal samples. They exhibit features described as 'diffuse bands' near the onset of the UV absorption, but the spectrum appears structureless at shorter wavelengths. Although weak absorption was observed at wavelengths longer than 240 nm [5,6], the contribution of 'hot bands' was not assessed.

In order to characterize the nature of the electronic state(s) responsible for the strong UV absorption, Blanchet and Stolow [9], and Suzuki and co-workers [10] measured time resolved photoelectron spectra following 210 and 200.5 nm excitation, respectively. Blanchet and Stolow [9] reported the existence of two time scales following excitation at 210 nm and proposed that a dark state reached by non-adiabatic transitions may participate in the dissociation. While the photoelectron spectrum associated with the NO dimer ion had a lifetime of about 300 fs, the corresponding spectrum associated with the $NO(X^2\Pi) + NO(A^2\Sigma^+)$ channel appeared at

* Corresponding author. Fax: +1-213-7403972.
E-mail address: reisler@usc.edu (H. Reisler).

0009-2614/$ - see front matter © 2004 Elsevier B.V. All rights reserved.
doi:10.1016/j.cplett.2003.12.092

longer times (lifetime $\sim$ 700 fs) [9]. On the other hand, Suzuki and co-workers found that at 200.5 nm the two time scales were comparable [10]. The latter investigators also concluded that the signature of the photoelectron spectrum obtained at early times was atypical of a Rydberg state converging to the ground state of the ion, and invoked the participation of a valence state in the 200–210 nm excitation region [10].

In the previous photoionization experiments, time resolved ion buildup and disappearance times were recorded by looking at both NO^+ and NO dimer ions. NO^+ appeared to be the major product in ionization of the NO dimer via the electronically excited state reached in the UV [10]. At these wavelengths, however, two competing processes can generate NO^+ ions. Ionization via the excited state of the dimer can access a dissociative state(s) of the ion, and/or the excited state of the neutral dimer can dissociate to produce $NO(A^2\Sigma^+)$, which is immediately ionized by the absorption of another photon. A problem in interpreting the results obtained with the femtosecond lasers at 200–210 nm was distinguishing clearly between NO^+ generated by dissociative ionization of the dimer and ionization of the $NO(A^2\Sigma^+)$ product.

In an attempt to further clarify the photochemistry and the nature of the excited state responsible for the strong absorption, we explored the region near and below the opening of the $NO(X^2\Pi) + NO(A^2\Sigma^+)$ channel. In our previous work, we have used molecular beams and photofragment ion imaging to explore the region just *above* the threshold of this channel (at 44,910 cm^{-1}) by excitation at wavelengths $\lambda \leqslant 223$ nm [11,12]. We concluded that the excited state is weakly bound, and that the predissociation dynamics was similar to that observed in weakly bound species, in that it exhibited restricted intramolecular vibrational redistribution (IVR) in the excited state. Specifically, the restricted IVR manifested itself as non-statistical $NO(A^2\Sigma^+)$ and $NO(X^2\Pi)$ product state distributions, particularly at the pair-correlated level.

In this Letter, we report the first study of the UV excitation of the NO dimer *below* the threshold of the $NO(X^2\Pi) + NO(A^2\Sigma^+)$ channel ($\lambda \geqslant 222.67$ nm), where NO^+ can only be generated via dissociative ionization of the dimer. For this study, we use a nanosecond excitation laser, and enlist the techniques of photoion and photoelectron imaging. We find that 1 + 1 resonance enhanced multiphoton ionization (REMPI) spectra of the NO dimer can be obtained by monitoring ions of both $m/e = 60$ (NO dimer ion) and $m/e = 30$ (NO^+ fragment). By scanning the wavelength of the excitation laser until the ion signal disappears, we place the onset of the UV electronic absorption at $\sim$ 41,300 (242 nm, 5.12 eV).

The low ion signal obtained near the onset of the absorption compared with the intensity at the peak indicates that the geometries of the ground and excited states of the neutral dimer differ considerably. The photoelectron kinetic energy (KE) distributions determined at several excitation energies in the region 242–223 nm are similar in shape to those obtained at early times using femtosecond lasers at $\leqslant 210$ nm [9,10]. The KE distribution is broad, indicating that the geometry of the excited state of the neutral dimer and the ground state of the ion are also quite different. This suggests that the 'bright' state has a valence, rather than a Rydberg, character.

Preliminary ab initio calculations carried out by Levchenko and Krylov for vertical excitation identify two strongly absorbing states (at $\sim$6.1 and 6.4 eV), which have a mixed valence/Rydberg character [13]. It is suggested that the valence state carries most of the oscillator strength in the Franck–Condon region, and that the evolution of this excited state(s) towards products leads eventually to the formation of the Rydberg $NO(A^2\Sigma^+)$ product, and (when enough energy is available) also the valence $NO(B^2\Pi)$ product.

2. Experimental details

The experimental arrangement has been described before [14], and only changes and improvements are elaborated here. $(NO)_2$ is generated in a molecular beam by supersonic expansion of gas mixtures containing 5–20% NO in He at a backing pressure of 2 atm. The rotational temperature in the beam is $T_{rot} = 3$–5 K [11]. The NO dimer is excited in a one-photon transition at wavelengths 242–221 nm generated by frequency-doubling the linearly polarized output of a Nd:YAG laser pumped dye laser system (Coumarin 440 and 480; 15–50 μJ; f.l. = 50 cm lens, $\tau_{pulse} = 5$–10 ns). The excited NO dimer is ionized non-selectively with a second photon at the same wavelength.

The ionization products, i.e., photoelectrons and ions with $m/e = 30$ and 60 (NO^+ and $(NO)_2^+$, respectively) are detected using the velocity map imaging technique [15]. The electrostatic lens design developed by Wrede et al. [16] is used. In this design, charged particles are formed in the region of a uniform electric field and accelerated before entering the focusing region. Such an arrangement narrows the relative velocity spread $\Delta v/v$, thereby significantly reducing the chromatic aberration of the electrostatic lens system. This is especially important in the work presented here, because both the photoelectrons and the NO^+ ions have broad kinetic energy distributions. The influence of external electric and magnetic fields is eliminated by use of μ-metal shielding around the ion optics and the time-of-flight region. A further improvement in resolution is achieved by using event-counting and centroiding [17,18].

In order to characterize the excited states of the NO dimer in the region 242–221 nm (5.1–5.6 eV), two types of experiments were performed. In the first, the laser wavelength was scanned throughout the whole region, and the total number of ions (event-counts) of $m/e = 30$ (NO^+) and 60 ($(NO)_2^+$), accumulated in 6000 laser shots, were recorded as a function of wavelength. In the second experiment, photoelectron and fragment NO^+ ion images were obtained at selected excitation energies. The two-dimensional (2D) projections were converted to 3D velocity distributions using the basis set expansion (BASEX) method [19]. The fragment and photoelectron speed distributions were derived in each case by analytical integration of the reconstructed images, expressed as linear combinations of basis functions, over all angles. The angular distributions were obtained directly from the expression of the images in polar coordinates.

Background subtraction was required only for photoelectron imaging. The source of background was photoelectrons produced by scattered light from the ion optics copper plates (work function = 4.7 eV). To minimize it, the experiments were performed in a series of short-time accumulations, one half of which done with the nozzle switched off. The 'nozzle off' images were then subtracted from the 'nozzle on' ones. In the detection of NO^+ ions, a minor contribution due to non-resonant ionization of the cold NO in the molecular beam was observed. However, this signal was less then 1% of the total NO^+, and therefore no background subtraction was required. Background due to non-resonant two-photon ionization of the NO dimer was minimized by using low laser fluences.

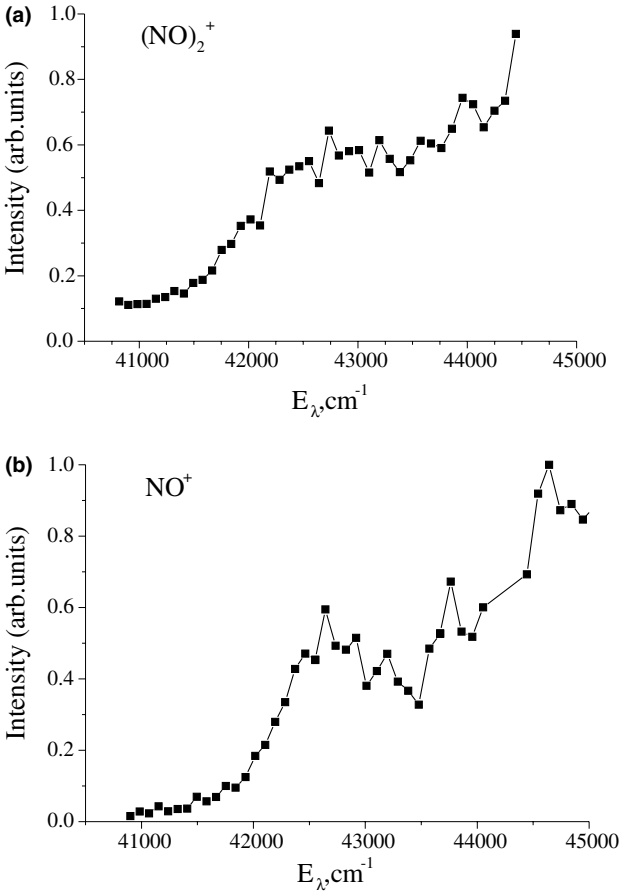

Fig. 1. Ion signals of (a) $(NO)_2^+$ and (b) NO^+ obtained in 1 + 1 REMPI of the NO dimer as a function of excitation energy. Typical error bars are ±20% of the signal intensity.

3. Results and discussion

Fig. 1a and b show the total $(NO)_2^+$ and NO^+ signal, respectively, as a function of excitation energy. There are three possible mechanisms for the production of NO^+ in our experiments: (a) non-resonant two-photon ionization of cold NO in the molecular beam; (b) 1 + 1 dissociative ionization of the NO dimer [$(NO)_2 + h\nu \rightarrow (NO)_2^+(v > 2) + e^- \rightarrow NO + NO^+ + e^-$] [20]; and (c) ionization of excited NO fragments produced by two-photon absorption in $(NO)_2$ followed by dissociation [$(NO)_2 + 2h\nu \rightarrow (NO)_2^{**} \rightarrow NO + NO^* \rightarrow NO + NO^+ + e^-$]. Under specific conditions, NO^+ ions produced via all three mechanisms were, indeed, observed in our experiments. As mentioned in Section 2, channel (a) contributes little to the total NO^+ signal. Moreover, ions produced via this mechanism are easily distinguishable, as they have zero translational energy and appear only at the center of the image. Two-photon absorption in the NO dimer with subsequent dissociation into electronically excited NO fragments [mechanism (c)] has been observed in a broad excitation range, and will be described in detail in a separate publication [21]. For the purpose of the present study, we emphasize that although channels (b) and (c) result in similar NO^+ translational energy distributions (with a large fraction of the ions having low KE), their corresponding photoelectron kinetic energy distributions are very different (see below). Therefore, the relative contributions of these two channels to the NO^+ yield can be estimated. Under our experimental conditions, mechanism (b) was found to be the dominant source of NO^+ fragments (see below). Thus, the plot in Fig. 1b represents primarily 1 + 1 dissociative ionization of the NO dimer. The similarity of the $(NO)_2^+$ and NO^+ yield curves reinforces this conclusion.

The origin of the lowest UV absorption band is estimated from the onset shown in Fig. 1 at 41,300 ± 300 cm^{-1} (242 nm, 5.12 eV). The absorption spectrum does not display reproducible narrow structures, indicating that the state excited initially is short-lived ($\tau \leqslant 100$ fs) and quickly dephases.

The $(NO)_2^+$ signal is much smaller compared to that of the NO^+ fragment, indicating that, even near the onset of the UV absorption, ionization via the excited

$(NO)_2$ state produces predominantly a dissociative state of the NO dimer ion, whose ground state is bound by ~5000 cm^{-1}. This implies that the Franck–Condon factors for the formation of vibrationally 'cold' ground state ions are unfavorable and that the geometry of the dimer's excited state differs significantly from that of the cation. In contrast, the ground states of the NO dimer and its cation have rather similar geometries [22–25], and direct ionization of the ground state dimer produces predominantly low vibrational levels of $(NO)_2^+$ and short vibrational progressions (2–3 bands) in the photoelectron spectrum [26]. These results have been reproduced in our experiments.

Fig. 2 shows a photoelectron image obtained at excitation wavelength $\lambda = 228$ nm (43,860 cm^{-1}), along with the photoelectron KE distribution. Fig. 3 shows the corresponding NO^+ image, and the ion KE distribution. The photoelectron KE distribution displays three distinct features. The major feature is broad and structureless, and its intensity increases as KE decreases. The signal starts to increase when the KE corresponds to the dissociative ionization channel. The angular distribution in this region is nearly isotropic.

The two narrow bands peaking at ~13,000 and 21,000 cm^{-1} are attributed to ionization of $NO(A^2\Sigma^+)$ and $NO(C^2\Pi)$, which are $n = 3$ Rydberg states generated via two-photon excitation/dissociation of $(NO)_2$ (mechanism (c) above). This assignment is confirmed by the dependence of the positions of the bands on photon energy. When the dissociative ionization process involves two photons (one for excitation of the dimer and one for dissociative ionization), the maximum KE of the photoelectrons must change as *twice* the photon energy. This is the behavior observed for the broad photoelectron feature. On the other hand, NO in a Rydberg state (produced by two-photon dissociation of the neutral dimer) requires only one photon for ionization and, therefore, the energy of the ejected photoelectrons should vary linearly with photon energy. Such one-photon energy dependence is observed for the two narrow bands. Also, with increasing laser power the intensities of the narrow bands increase relative to the broad feature, supporting the two-photon nature of the excitation process. At low laser power, the integrated intensity of the two narrow bands is eight times smaller than that of the broad feature, but we are unable to

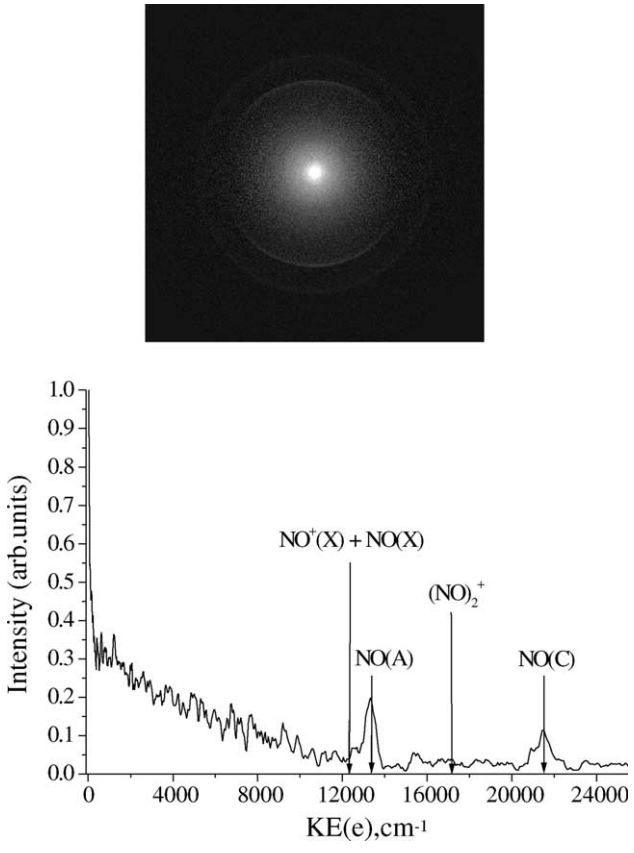

Fig. 2. Photoelectron image and the corresponding KE distribution obtained by 1 + 1 REMPI of the NO dimer at 228 nm. The arrows indicate the energetic thresholds for the formation of $(NO)_2^+(X, v = 0)$ and $NO^+(X, v = 0) + NO(X, v = 0)$, as well as the calculated positions of the photoelectron peaks corresponding to the ionization of NO(A) and NO(C) products (see the text for details).

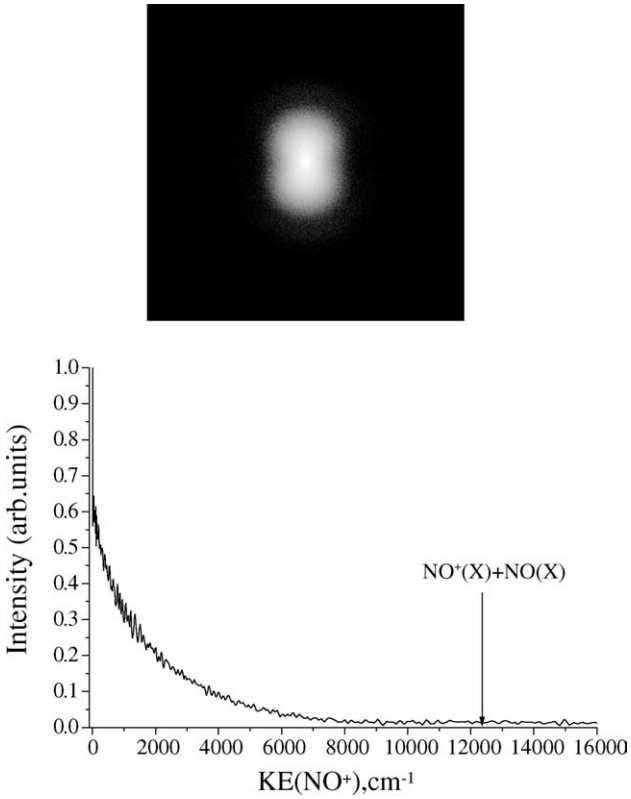

Fig. 3. Ion image and the corresponding KE distribution of NO^+ fragments resulting from the dissociative ionization of the NO dimer at 228 nm. The maximum available KE for this process (12,295 cm^{-1}) is marked with an arrow.

completely suppress these peaks due to poor signal/noise level at low laser intensities. Pursuant to the above, we believe that the major source of NO^+ in our experiment is the dissociative ionization of the NO dimer [mechanism (b)]. The signal of photoelectrons with KEs exceeding the dissociative ionization threshold, i.e., those corresponding to the formation of stable bound states of $(NO)_2^+$, is very small. This observation agrees with the low $(NO)_2^+$ signal observed in the ionization.

Referring to Fig. 3, the NO^+ KE distribution shows that the fraction of ion fragments formed with high KE is very small. In other words, the dissociation of the NO dimer cation by 1 + 1 ionization of the neutral produces highly vibrationally excited NO and/or NO^+ fragments. It is likely that these ions are generated by vibrational predissociation of ground state $(NO)_2^+$, but the participation of an electronically excited state of the ion cannot be precluded.

At wavelengths $\lambda \leqslant 222.67$ nm (44,910 cm^{-1}), i.e. above the threshold for production of $NO(A^2\Sigma^+)$ by one-photon dissociation of $(NO)_2$, both the photoelectron and NO^+ KE distributions change dramatically. A typical photoelectron image and the corresponding KE distribution obtained at $\lambda = 221.67$ nm (45,110 cm^{-1}) are shown in Fig. 4. A strong signal deriving from ionization of $NO(A^2\Sigma^+)$ is dominant in the spectrum, while almost no photoelectrons originating in the dimer ion are detected. In the corresponding NO^+ ion images, only fragments with low KE ($\leqslant 200$ cm^{-1}), which are correlated with one-photon dissociation of the NO dimer $[(NO)_2 + h\nu \rightarrow NO(A^2\Sigma^+) + NO(X^2\Pi)]$, are observed. Their KE distribution is similar to our previously published results [12].

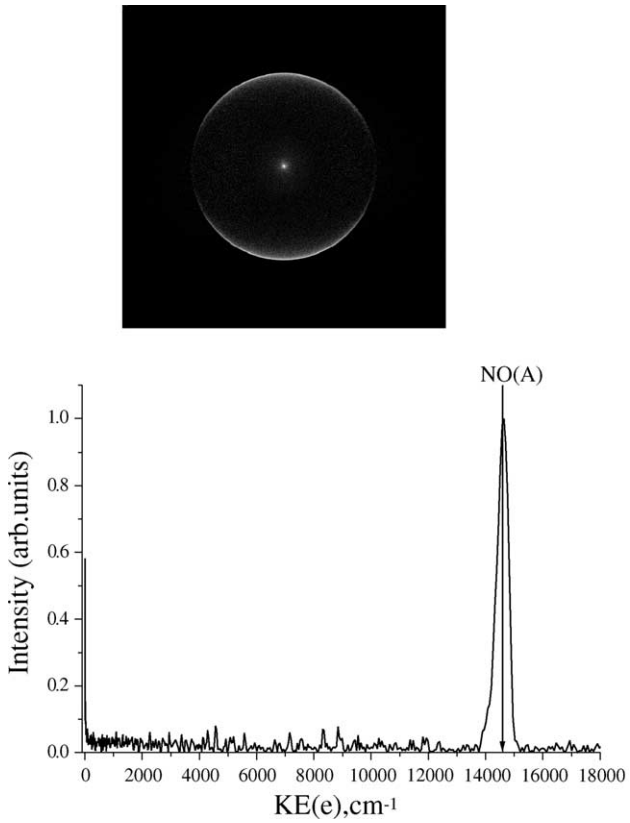

Fig. 4. Photoelectron image and the corresponding KE obtained following excitation of $(NO)_2$ at 221.67 nm. The large peak corresponds to ionization of $NO(A^2\Sigma^+)$ produced in one-photon dissociation of the NO dimer $[(NO)_2 + h\nu \rightarrow NO(A^2\Sigma^+) + NO(X^2\Pi)]$.

In the 200.5 and 210 nm measurements carried out with femtosecond lasers *at zero pump-probe delay* [9,10], the photoelectron and ion KE distributions are similar to the ones observed in our experiments at $\lambda \geqslant 222.67$ nm. This similarity suggests that the same 'bright' state is predominantly accessed at all wavelengths, but with nanosecond lasers the efficiency of ionizing the dimer when fast dissociation to $NO(A^2\Sigma^+)$ + $NO(X^2\Pi)$ is allowed is very small.

Additional insight into the nature of the excited state(s) can be obtained from preliminary ab initio calculations carried out by Levchenko and Krylov [13]. An EOM-CCSD study of the excited states of $(NO)_2$ using the 6-311(2+, 2+)G** and 6-311(2+, 2+)G(2df,2pd) basis sets shows the presence of only two states with large oscillator strengths in the region above 5 eV (5.0–8.5 eV). These states are composed primarily of two configurations, corresponding approximately to two 'diabatic' states: (i) a diffuse $3p_x$ Rydberg state (where the x-axis lies along the N–N bond), and (ii) a tight valence state of the same symmetry. The vertical excitation energies to the adiabatic states are 6.1 and 6.4 eV, and the oscillator strengths are ~0.45 and ~0.2, respectively. These values are 2–3 orders of magnitude higher than those of any other state in this region. Thus, we propose that the bright state at 6.1 eV vertical excitation contributes considerably to the observed absorption at the lower energies examined in this work (~5.2 eV). The B_2 symmetry of the two states explains the observed parallel nature of the absorption in the region of 222–193 nm (5.57–6.43 eV) [11,12,27].

The calculated values of the oscillator strengths for these two states are considerably higher than expected for pure Rydberg states, which rarely exceed 0.08 [28]. They are more typical of excitation to valence states, whose oscillator strengths often reach values of 0.3–1.0. Therefore, the valence rather than the Rydberg component in both states is likely responsible for the 'bright' character. The nature of the valence state and the origin of the strong mixing of this state with the 3p-Rydberg state are not yet known. It is noted, however, that strong UV emission from the valence $NO(B^2\Pi)$ product is observed following 193 nm dissociation, and this channel may be related to the valence component of the dimer excited state. More theoretical work is needed to better understand the nature of the excited states of the dimer in this energy region and to elucidate the role of

non-adiabatic transitions in dissociation terminating in $NO(A^2\Sigma^+) + NO(X^2\Pi)$.

4. Conclusions

The 1 + 1 REMPI spectrum of the NO dimer was studied below the opening of the NO(X) + NO(A) channel via velocity map imaging detection of photoelectrons and NO^+ and $(NO)_2^+$ ions. The origin of the lowest excited state of the NO dimer in the UV region is at 5.12 ± 0.04 eV (242 ± 1 nm; $41{,}300 \pm 300$ cm^{-1}). The absence of narrow structures in the absorption spectrum is probably due to fast dephasing processes in the excited state. Nevertheless, the excited state lives long enough to be ionized by absorption of another photon. This ionization accesses a predominantly dissociative state of the NO dimer cation, suggesting that the excited state has a large valence component. The broad photoelectron spectrum indicates that the geometries of the excited neutral dimer and the dimer ion are quite different. The photoelectron and ion KE distributions are similar to those reported by other research groups following excitation at 210 nm (5.90 eV) and 200 nm (6.20 eV) and imply that mainly one 'bright' state is accessed at all wavelengths. These conclusions are in agreement with preliminary ab initio calculations, which reveal a mixed valence/Rydberg (p_x) state having a large oscillator strength.

Acknowledgements

Support by the National Science Foundation and the Donors of the Petroleum Research Fund, administered by the American Chemical Society is gratefully acknowledged. The authors thank Toshinori Suzuki, Albert Stolow, Carl Hayden, and James Shaffer for helpful discussions and sharing of unpublished results on time-resolved photoelectron and photofragment measurements of NO dimer dissociation.

References

[1] J.R. Hetzler, M.P. Casassa, D.S. King, J. Phys. Chem. 95 (1991) 8086.
[2] E.A. Wade, J.I. Cline, K.T. Lorenz, C. Hayden, D.W. Chandler, J. Chem. Phys. 116 (2002) 4755.
[3] A.L.L. East, J. Chem. Phys. 109 (1998) 2185.
[4] R. Sayos, R. Valero, J.M. Anglada, M. Gonzalez, J. Chem. Phys. 112 (2000) 6608.
[5] J. Billingsley, A.B. Callear, Trans. Faraday Soc. 67 (1971) 589.
[6] E. Forte, H. Van Den Berg, Chem. Phys. 30 (1978) 325.
[7] O. Kajimoto, K. Honma, T. Kobayashi, J. Phys. Chem. 89 (1985) 2725.
[8] Y. Naitoh, Y. Fujimura, O. Kajimoto, K. Honma, Chem. Phys. Lett. 190 (1992) 135.
[9] V. Blanchet, A. Stolow, J. Chem. Phys. 108 (1998) 4371.
[10] M. Tsubouchi, C.A. de Lange, T. Suzuki, J. Chem. Phys. 119 (2003) 11728.
[11] A.V. Demyanenko, A.B. Potter, V. Dribinski, H. Reisler, J. Chem. Phys. 117 (2002) 2568.
[12] A.B. Potter, V. Dribinski, A.V. Demyanenko, H. Reisler, J. Chem. Phys. 119 (2003) 7197.
[13] S.V. Levchenko, A.I. Krylov, private communication.
[14] A. Sanov, Th. Droz-Georget, M. Zyrianov, H. Reisler, J. Chem. Phys. 106 (1997) 7013.
[15] A. Eppink, D.H. Parker, Rev. Sci. Instrum. 68 (1997) 3477.
[16] E. Wrede, S. Laubach, S. Schulenburg, A. Brown, E.R. Wouters, A.J. Orr-Ewing, M.N.R. Ashfold, J. Chem. Phys. 114 (2001) 2629.
[17] Y. Tanaka, M. Kawasaki, Y. Matsumi, H. Fujiwara, T. Ishiwata, L.J. Rogers, R.N. Dixon, M.N.R. Ashfold, J. Chem. Phys. 109 (1998) 1315.
[18] B.-Y. Chang, R.C. Hoetzlein, J.A. Mueller, J.D. Geiser, P.L. Houston, Rev. Sci. Instrum. 69 (1998) 1665.
[19] V. Dribinski, A. Ossadtchi, V.A. Mandelshtam, H. Reisler, Rev. Sci. Instrum. 73 (2002) 2634.
[20] S.H. Linn, Y. Ono, C.Y. Ng, J. Chem. Phys. 74 (1981) 3342.
[21] V. Dribinski, A.B. Potter, I. Fedorov, H. Reisler, unpublished results.
[22] S.G. Kukolich, J. Mol. Spectrosc. 98 (1983) 80.
[23] A.R.W. McKellar, J.K.G. Watson, B.J. Howard, Mol. Phys. 86 (1995) 273.
[24] A.L.L. East, J.K.G. Watson, J. Chem. Phys. 110 (1999) 6099.
[25] Y. Xie, H.F. Shaefer III, X.-Y. Fu, R.-Zh. Liu, J. Chem. Phys. 111 (1999) 2532.
[26] I. Fisher, A. Strobel, J. Staecker, G. Niedner-Schatteburg, K. Muller-Dethlefs, V.E. Bondybey, J. Chem. Phys. 96 (1992) 7171.
[27] Y. Naitoh, Y. Fujimura, F. Honma, O. Kajimoto, J. Phys. Chem. 99 (1995) 13652.
[28] M.B. Robin, Higher Excited States of Polyatomic Molecules, Academic Press, New York, 1974.